

Advanced system for calibration and characterization of solar cells

F. GRANEK and T. ŻDANOWICZ*

Faculty of Microelectronic Systems and Photonics, SolarLab, Wrocław University of Technology
11/17 Janiszewskiego Str., 50-372 Wrocław, Poland

This paper presents high performance setup developed at the SolarLab to measure current-voltage (I–V) curves of solar cells. The core of a setup is a steady light solar simulator of class A, according to specifications of IEC 60904-9 and ASTM E927 standards. Available range of measurements enables us to characterise not only all kinds of silicon wafer-based solar cells but also thin film cells and minimodules. A lot of effort has been done to make a setup as a powerful tool for advanced research work. For that purpose, such options have been implemented as various algorithms for I–V curve translation to external conditions other than those recorded during measurement or several techniques to determine lumped series resistance of solar cells (in both cases procedures recommended by IEC 60891 standard have been included). Advanced numerical fitting algorithms allow to extract from I–V curves the parameters corresponding to either of three commonly used equivalent diode models of a solar cell.

Using an independent microprocessor unit, the temperature of the measuring table may be controlled in the range 0–60°C due to a system of four Peltier cells attached to its rear side. This allows for routine determination of thermal coefficients of basic cell parameters.

The paper discusses also some of elemental random and nonrandom error sources that can be encountered during the standard I–V measurements of a solar cell. The test results of repeatability of measurements, problems related to probe configuration, and heating up of the cells during “light” measurements are presented showing that the developed system can be successfully used both for laboratory work and as a tester on a production line. The system meets all requirements of the IEC 60904-1, IEC 60904-3, and IEC 60904-9 standards.

Keywords: I–V curve, solar cell calibration, solar cell characterisation.

1. Introduction

Characterisation of solar cells is an equally important task both on a production line during manufacturing process as well as during research work in a laboratory. However, there may be quite different requirements concerning either accuracy and/or speed of the measurements. And so, during on-line tests high accuracy may not be of the primary importance yet the measurement rate and repeatability usually remain critical if one takes into account typical production throughput usually well exceeding 1000 cells/hour. Contrary to that, in a course of research work, high accuracy and good control and repeatability of the measurement conditions rather than speed may be crucial for proper recognition and analysis of the physical features of the characterised device. The speed of measurement is significant as far as it may affect the final result of test itself, e.g., due to a change of temperature or finite photo-current response time of the device.

At the SolarLab, effort has been done to develop a system for characterisation of the solar cells in, so-called, standard test conditions (so-called STC, i.e., light spectrum

AM1.5G, normalised to 1000 W/m² and 25°C cell temperature) in accordance with the requirements of IEC 60904-1 [1] and IEC 60904-3 [2] standards and with variety of options implemented that may be helpful in advanced research work. Other aim was to combine high accuracy of the measurement with repeatability and speed that would make the setup suitable for cell manufacturing as well. Many of tests have been performed on the setup to recognise and present possible random or nonrandom sources of errors that can be encountered during standard I–V curve scans.

2. System description

2.1. Solar simulator

Light source is a core of each system for PV device characterisation. It should meet several requirements such as proper spectral distribution of the emitted light, long and short time stability of its intensity and acceptable irradiance uniformity over the area provided for positioning of a cell for test. In the case the spectrum of the light resembles closely enough spectral distribution of the natural solar radiation then such equipment is called solar (or sun) simula-

*e-mail: zdanowic@pwr.wroc.pl

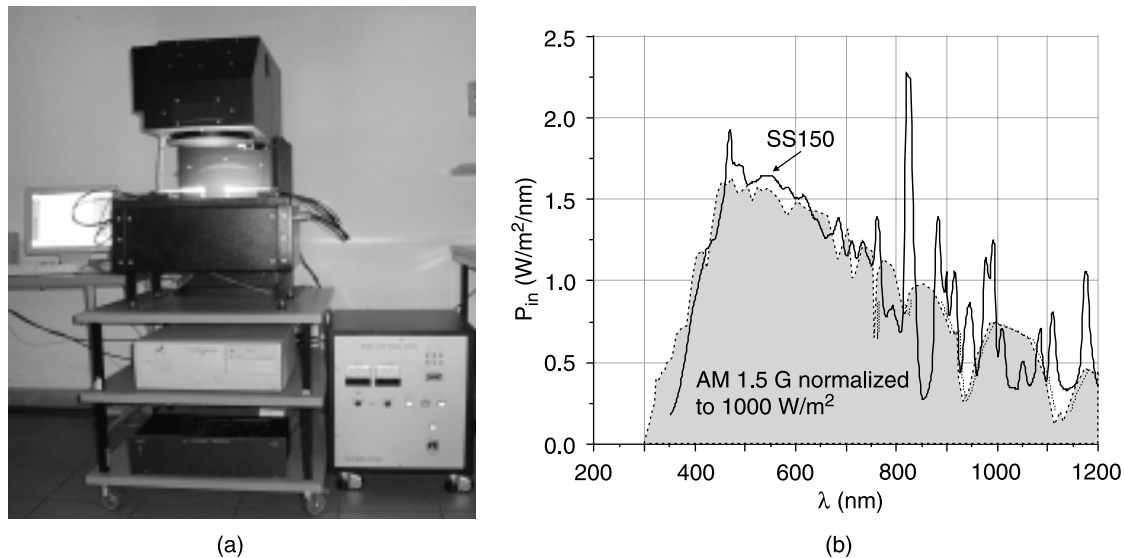


Fig. 1. General view of the complete system developed at the SolarLab: spectral distribution of SS150 Solar Simulator superimposed on AM1.5G standard spectrum normalised to 1000 W/m^2 [2] (a), measurement was carried out at the SolarLab using optical spectrum analyser AQ-6315B of Ando Electric Co. Ltd. (Japan) (b).

tor. In SolarLab system, continuous light solar simulator of the type SS150 of the Photoemission Techn. Inc. (USA) with short arc xenon lamp as a light source has been used. The equipment may be classified into the highest A-class category according to the requirements of the IEC 60904-9 standard [3]. Figure 1 shows a general view of the SolarLab's setup together with the spectral distribution of light emitted by SS150 solar simulator as compared to AM1.5G standard distribution [2]. The measurements were carried out at the SolarLab using optical spectrum analyser AQ-6315B of the Ando Electric Co. Ltd. (Japan). The measured curve is in a very good agreement with the test data delivered by the equipment manufacturer. The illuminated area of the guaranteed uniformity is $15 \times 15 \text{ cm}^2$ for SS150 which is in practice, with only few exceptions, the largest area of most crystalline silicon commercial solar cells available on the market today.

2.2. Measuring setup

An electronic circuit used to measure I–V curves of solar cells was developed solely at the SolarLab (Fig. 2). It consists of the voltage controlled power supply with “operational amplifier type” output what means that the current may flow through it in both directions thus enabling taking I–V curve of the illuminated cell in three quadrants. Maximum output current has been designed for $\pm 20 \text{ A}$ which is value roughly three times higher than short-circuit current I_{SC} of the typical $15 \times 15 \text{ cm}^2$ Si cell. This feature may be especially useful when measuring ‘dark’ curves of a cell biased far in the forward direction. Maximum voltage range designed for 10 V makes possible to characterise, apart of standard cells, also non-standard PV devices like thin-film minimodules. Current is measured as a voltage drop on one of the set of seven

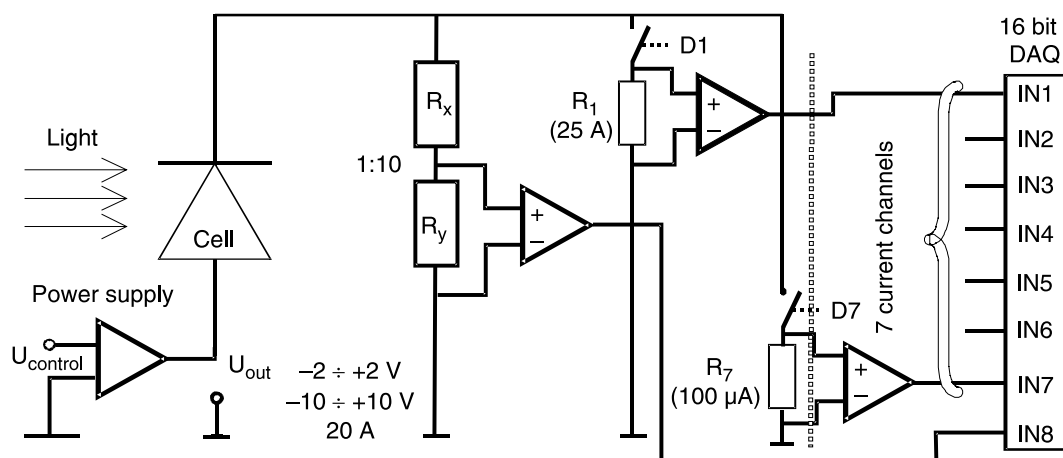


Fig. 2. Electrical scheme of the SolarLab's system for I–V curve measurements of the solar cells. Seven resistors for current measurement settle seven ranges for current measurements ($100 \mu\text{A}$ – 25 A) each using separate input of the 16-bit DAQ PC card. The output voltage of the power supplier is controlled using the 12-bit D/A converter and current ranges are changed using binary output signals of the same card, respectively.

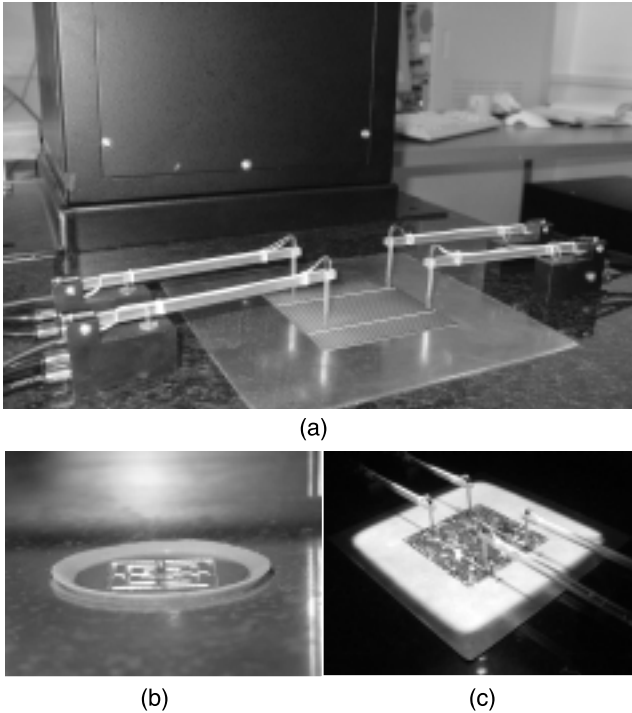


Fig. 3. Measuring brass table with a set of four soft-touch gold-plated vacuum controlled probes: gasket made of extra soft silicone rubber enabling effective sucking to the table cells having non-perfectly smooth (or even soldered) surface of the rear side (a), view of the table during “light” measurement of a standard $10 \times 10 \text{ cm}^2$ multi-Si solar cell with well visible shadowing of the cell’s active area introduced by non ideally transparent polycarbonate arms of the measuring probes (b), note that though square-like spot light has dimensions $\sim 20 \times 20 \text{ cm}^2$ yet only area limited to $15 \times 15 \text{ cm}^2$ with uniformity of light intensity specified for class A [3] is available for high quality measurements (c).

high precision resistors ranging from $2 \text{ m}\Omega$ to 500Ω . To avoid excessive number of relays and undesired voltage drops in the current measuring circuit seven independent signal lines have been provided each connected to different input of a 16 bit DAQ card in the PC computer. Opening the current circuit (all relays open) allows for direct measurement of then open circuit voltage V_{OC} of a cell.

A measuring table and probes were designed to perform measurements in classic four wire Kelvin configuration with simple vacuum based control of the probes movement. Massive brass table ($\sim 6 \text{ kg}$) with a polished surface plays a role of current probe contacting to a rear side of the measured cell (Fig. 3). It plays also another important role as a heat sink stabilising the cell’s temperature during a measurement. Two voltage probes contacting rear side of the cell are located inside the table (galvanically isolated from the table). They are moving up at the same moment the measured cell is being sucked to the table. Both voltage as well as current “soft touch” telescopic probes are gold-plated and their movement is controlled either by TTL signal from the computer or by pressing a foot-pedal. Four probes contacting to front metallisation of the cell are independently positioned making simple to measure the cells of any size and pattern of the metallisation grid. To reduce shadowing introduced by upper probes during “light” measurements, their arms have been done of the highly transparent polycarbonate material. Special gasket made of very soft silicone rubber [Fig. 3(b)] provides good electrical contact to the table and firm measurement of the cells which are not perfectly smooth on their rear sides or even have been earlier soldered for further mounting in PV modules.

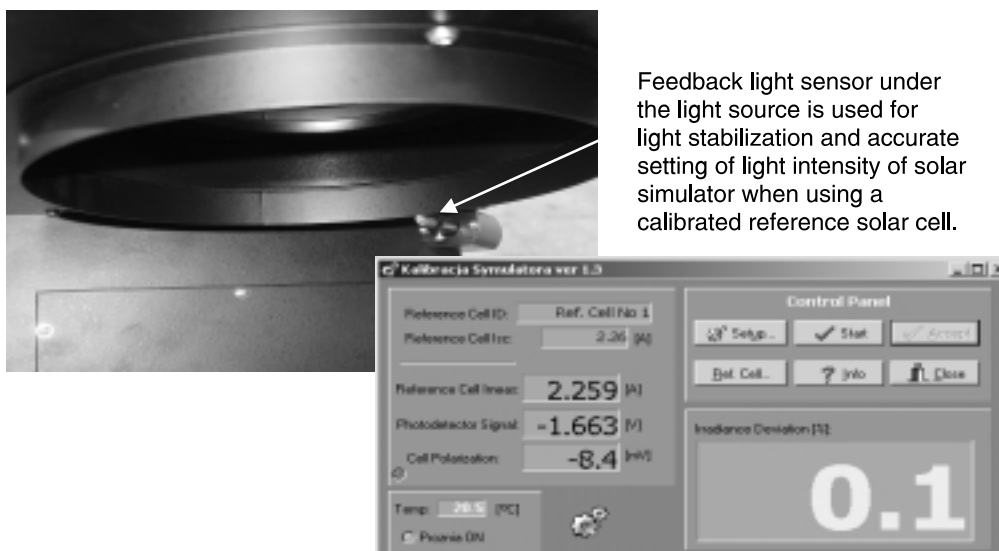


Fig. 4. Window showing procedure developed for accurate adjustment of light intensity on the surface of the measurement table with use of solar cell that was calibrated in a certified laboratory; high stability of irradiance allows operator easily to set required light intensity with resolution as good as shown in the figure; during read out of the short-circuit current the reference cell is biased possibly close to “zero” voltage (-8.4 mV for the case shown in the figure); value of the photodiode signal (here -1.663 V) is stored in configuration file and then used to determine actual irradiance level during further measurements.

2.3. Setting light intensity and stability control

SS150 solar simulator provides two optional modes of light intensity control by applying different control signals in the feedback loop of the power supply. The first of these options stabilises the lamp's current using a signal from a current sensor while the other stabilises directly light intensity using for control a signal coming from a photodetector mounted under the light source. While in the current mode light is stabilized on the level not better than 1%, which is not good enough for accurate measurements, yet in the light control mode both long-term as well short-term stability of the light intensity may be even better than $\pm 0.15\%$ (see example in Fig. 7, Sect. 3.3).

Figure 4 illustrates how the signal from the photodetector has been applied in the procedure developed for accurate setting of the intensity level with use of a reference solar cell.

3. Light measurements

3.1. Opening the shutter of the light source

When the light output of SS150 is closed by a mechanical shutter, the power supply generates a current which is about 80% of the lamp's rated value. After opening the shutter, the light intensity starts to be controlled using signal generated by a photodetector (Sect. 2.3.) To determine what is time delay necessary to open the shutter and stabilise the light intensity at the required level, V_{OC} of the cell positioned in the table was sampled immediately after sending from PC the signal opening the shutter. Figure 5 shows the result of this experiment. Two characteristic points (marked A and B, respectively) could be noted. At

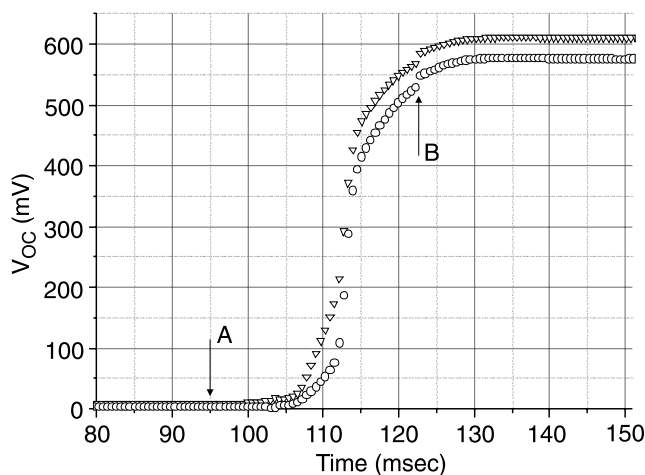


Fig. 5. Change of V_{OC} of two different cells positioned within illumination area measured to determine time delay necessary to start scan of I–V curve after sending control signal to open lamp's shutter. Point A is a moment when shutter starts to open and at the time marked as point B control over light intensity is taken by photodetector (see Fig. 3); minimum time delay necessary before measurement may be started is about 160 ms.

point A, after about 90–95 ms, the shutter starts to open and after next 35–40 ms (point B) when the photodetector already “sees” a light beam, the control mode is “switched on” resulting in distinct increase in light intensity. As it can be clearly seen in Fig. 5, the system needs additional a few tens of milliseconds to reach required level of the light intensity. It means that in total at least 140–150 ms of time delay are necessary before I–V scan may be finally started.

3.2. Heating up of the cell by irradiation beam

One of the frequently claimed disadvantages, when using continuous light solar simulators, is an effect of undesired and, what even worse, uncontrolled rise of the cell's temperature due to a relatively long time of I–V curve scan. Since the best indication of the true cell's junction temperature is its V_{OC} [4], the same scheme of experiment as described in previous section was used to verify this opinion. In Fig. 6(a), the data showing difference between actual and maximum value of V_{OC} measured after sending a signal to open the shutter have been plotted for the cells of various size and thickness. The data cover the range from 100 ms up to 500 ms which is typical range of scan duration in the system. As it can be seen, the cells marked as 3 and 7 (old Astropwer's single crystal Si cells) showed the most pronounced heating up effect. Both cells were the thickest ones ($> 500 \mu\text{m}$) and cell no. 3 was additionally soldered to 1.5 mm thick printed board glassy laminate this way being in practice thermally isolated from the measuring table. In the case of cell no. 7, the characteristic feature that could significantly limit heat transfer to brass ‘sink’ was that the cell had only two relatively thick silver bus bars printed over strongly oxidised Al layer on the rear side. Most probably this was the main reason for rather poor thermal contact of the cell to the measuring table even when it was vacuum sucked. Quite similar situation was in the case of Koycera cell marked as no. 4. The cell was soldered on both sides by manufacturer and silicone gasket had to be used to suck it firmly to the table. Apparently poor thermal contact to the table was provided in this case only through the narrow bars of solder on the rear surface of the cell. Contrary to described cells, the IMEC's cell – marked as no. 1 – of about $350 \mu\text{m}$ thickness had a rear surface entirely covered by a very smooth silver layer thus ensuring the best possible thermal contact to the table. This caused that temperature of this cell increased less than 1°C during 500 ms. All other cells (marked as 2, 5, and 6) had silver grid pattern printed on the back side. They showed V_{OC} drop in the range 2–3 mV corresponding to increase in the temperature in the range of 1.0 – 1.5°C . Basing on the presented results it may be concluded that a type of the cell's substrate, either single crystal or multicrystalline, or its thickness, has not significant influence on the rate of the observed heat up effect. Even in the case of the very thin ($\sim 170 \mu\text{m}$) multicrystalline cell from Photowatt (no. 5) the effect was very similar to that observed for other much thicker cells. The crucial factor having an influence on the

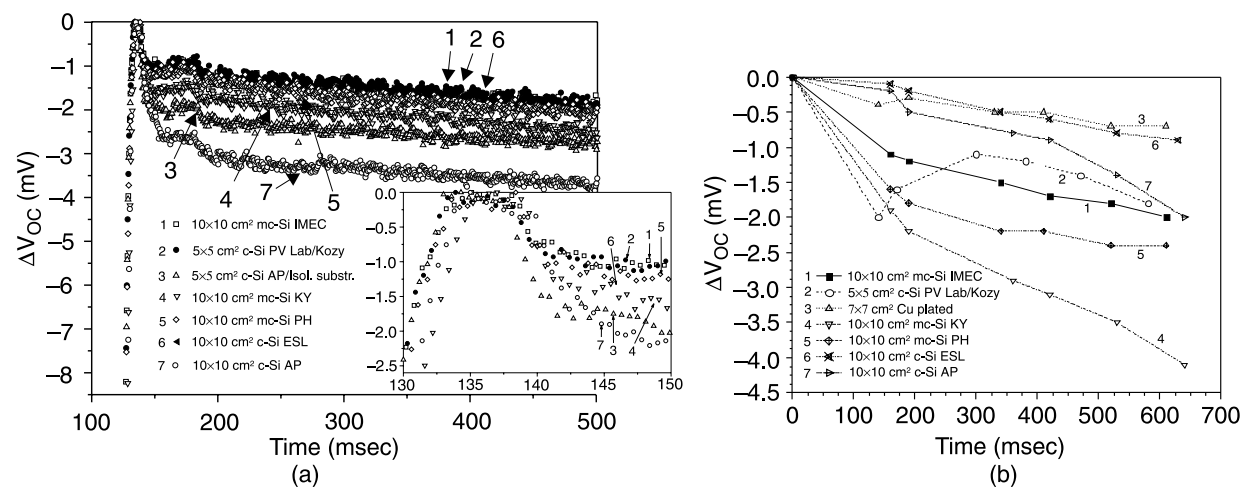


Fig. 6. Change of V_{OC} for various cells positioned within illumination area measured after opening the shutter of the solar simulator to determine possible effect of cell's heating up due to absorbed radiation. V_{OC} was measured either directly (a) or determined from the I-V curve and plotted as function of scan duration (b); in both cases as a reference to calculate V_{OC} change 'plateau' value shown as insert figure in (a) was used; within reasonable accuracy limits it may be assumed that 2 mV drop in V_{OC} corresponds to increase in the cell's junction temperature by 1°C. The meanings of the symbols in the label refer to cell manufacturer as follow: AP – AstroPower (USA), IMEC (Belgium), ESL – Electroscience Lab. (USA), KY – Kyocera (Japan), PV Lab/Kozy – Photovoltaic Lab. Kozy (Poland), PH – Photowatt (France), Cu plated – manufacturer unknown.

discussed effect seems to be the quality of the thermal contact between the cell and the measuring table.

To confirm this conclusion, the measurements were repeated but this time V_{OC} values were extracted from the I-V characteristics. In Fig. 6(b), the data showing the difference between V_{OC} and the maximum value of V_{OC} corresponding to "plateau" region [insert in Fig. 6(a)] have been plotted as a function of the scan duration. A time delay for opening the shutter has been set for 300 ms. Additionally, there have been plotted the data for the cell with Cu contact plated over the entire rear side. For this cell, V_{OC} decreased only by 0.7 mV after 600 ms scan duration confirming the effectiveness of a thermal contact between the cell and the measuring table. As it can be seen for all other cells, except that of Kyocera one, an error in V_{OC} due to heat up effect was limited to about 2 mV up to 400 ms of the scan duration.

3.3. Duration of I-V curve scan

As it was pointed out earlier, duration of the measurements may be important factor in the case of the production on-line tests and/or due to possible cell's heat up effect. Figure 7 presents example of I-V measurement practically limited to only one I-V quadrant in order to minimise scan duration. Such kind of a fast measurement may be recommended for on-line tests when determination of only basic cell's parameters is necessary. Wider range of a measurement may be advisable when the further analysis of the curve is planned, e.g., for determination of the cell's internal parameters (see Sect. 3.6).

To check if the scan rate may affect the shape of I-V curve a lot of measurements with cell's bias changing in both directions during the scan have been carried out for a wide range of scan rates. Final scan duration time changed

from about 120 ms up to more than 1000 ms. As it was expected the applied scan rates were too low to cause any noticeable hysteresis in the measured characteristics.

3.4. Positioning of measuring probes

It is well known that both number of probes as well as their location on the bus bars of the cell's front electrode may significantly affect the shape of the measured I-V curve. This is mainly due to voltage drop on the series resistance

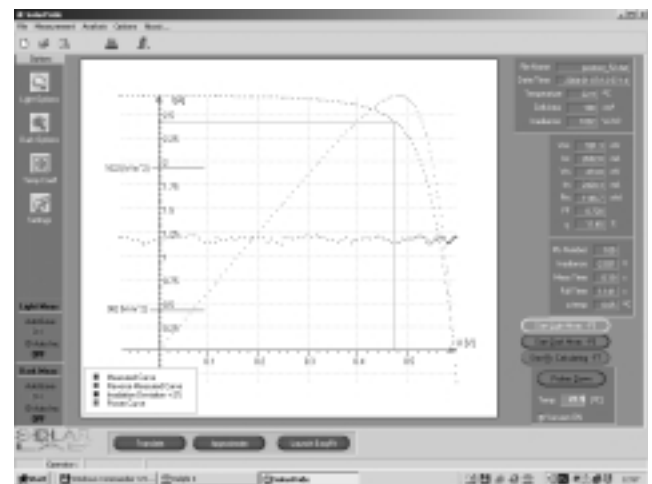


Fig. 7. Example of fast "light" measurement carried out for set of options resulting in scan duration 0.19 s (105 I-V points measured); note that thereby to calculate whole duration time about 0.55 s provided for cell sucking and probes adjustment as well as 0.3 s to open the shutter must be added; dotted line plotted close to the middle of the graph shows fluctuations of the light intensity during the scan within marked 2% range of the preset level.

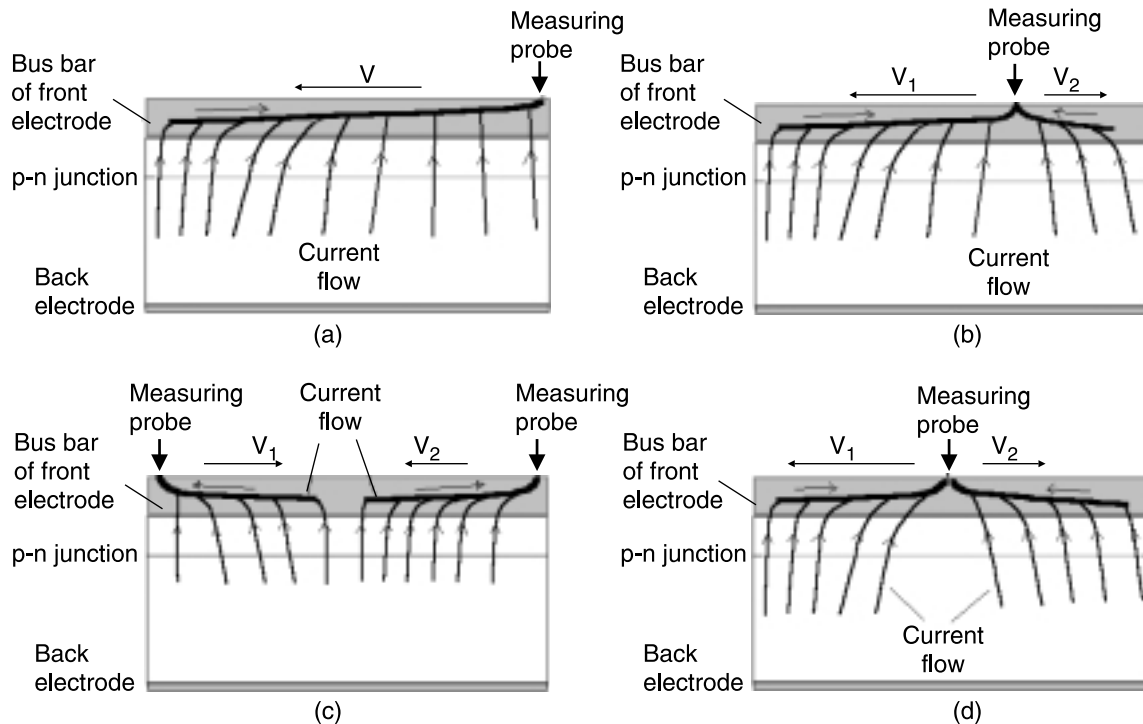


Fig. 8. Schematic pattern of the current flow through the bus bar of a standard solar cell's front metallisation during I-V curve measurement for different configurations of the measuring probes: asymmetrical position of single probe close to the edge of a cell a); asymmetrical position of single probe between centre and the edge of a cell resulting in reduced effect of the series resistance (b); two symmetrical positioned probes (c); single probe positioned in the centre of a cell (d). Components of voltage drop due to finite spread resistance of the metallisation has been marked for each case; note that in the case of "symmetrical" configuration of probes as presented in Figs. (c) and (d), voltages V_1 and V_2 have the same values but opposite signs due to 'splitting' of the current into two equal streams.

of the non-soldered bus bars and – though too much lower extent – nonuniform distribution of photocurrent generated in a cell and then flowing to its front electrode [5].

Typically, before mounting in PV module, the cells are tabbed and thus series resistance of the electrode's bus bars being practically eliminated. Because of that it is advisable to measure solar cell in such way thereby to avoid effect of the resistance of the bus bars on the I-V curve shape, especially if the cell has not been taped nor/and soldered yet.

To meet this requirement the setup developed at the SolarLab has been provided with the set of four probes to contact the cell's upper electrode. Using only two probes, asymmetrically positioned at the same edge of the cell (in majority of today manufactured cells, front grid metallisation consists of two parallel bus bars) as is schematically shown in Fig. 8(a), causes that actual cell bias is decreased by the entire voltage drop on the bus bar. Since the cell's contact areas are usually located close to one of its edges, hence such configuration of probes imitates well a situation of a cell mounted in a PV module. This mode of measurement may be thus recommended for already tabbed and/or soldered cells. However, if the cells with still "bare", either thin-film or thick-film front metallisation, are to be characterised, then symmetrical probe configuration should be used [Fig. 8(c)]. In such a case, approximately the same amount of current flows through the bus bar to each probe and then to external circuit. These current com-

ponents give equal voltage drops on the electrode yet having opposite signs [Fig. 8(c)]. This way, the possible impact of the series resistance of the cell's electrode on the shape of I-V curve may be eliminated. Similar situation would take place if only one pair of probes, but positioned

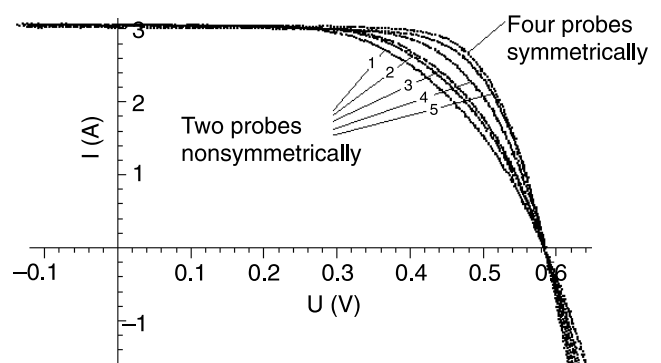


Fig. 9. I-V plots measured for probes configuration from Fig. 8 showing effect of a series resistance introduced by bus bars of the cell's front electrode; note that curve no. 5 which was measured with only two probes located close to centre of a cell does not differ much from the curve measured with all four probes. Because of I_{SC} reduction due to shadowing effect [see Fig. 3(c) and comments] all curves measured with only two probes were corrected using Blaesser's receipt [7,8] to keep I_{SC} value the same as in the case of measurement with four probes located as close as possible to the edges of the cell to minimise shadowing.

in the centre of the cell, were used [Fig. 8(d)]. Figure 9 shows the results of I–V measurements for various configurations of the probes – with all four probes as well as with only two probes positioned in different points of a cell’s bus bars.

3.5. Translation of I–V curves to standard test conditions (STC)

There are three numerical formulas most commonly used for translation I–V curves of PV devices to STC if the conditions during measurement differed from those required ones. One of these formulas has been published as IEC 60891 standard [6]. The other two have been developed by Blaesser from JRC [7] and Anderson from NREL [8], respectively. These procedures are particularly useful in case when I–V characteristics of PV devices – mainly PV modules and/or PV arrays – have been measured in outdoor conditions where STC can be hardly met [8]. Contrary to that, in case of indoor measurements, when one may expect only small deviations from standard conditions, the translation procedures are used rather as a curve “correction” tool. A possible error due to such slight correction is usually negligible [9] making such option, when implemented in the software of the test system, very convenient tool for translation of those I–V curves that were measured in the conditions only slightly different from STC which is quite typical situation for indoor measurements.

In SolarLab’s system, all the three above mentioned formulas have been implemented and they may be used either “off hand” or automatically immediately after I–V measurement has been finished.

3.6. Fitting cell’s parameters to equivalent model

Fitting I–V curve to any of several existing equivalent models of a PV device is important mainly for the analysis of physical properties of a cell at different temperatures and irradiance conditions. It can be also useful tool for determi-

nation of the cell’s shunt and series parasitic resistances. Description of numerical basics of I–V curves fitting together with most important equivalent circuits of PV devices may be found in Ref. 10. The procedures described therein have been implemented in the SolarLab’s system and fitting of the I–V characteristic may be done directly after the measurement has been completed or after loading I–V data stored earlier on the PC’s hard disk.

Usefulness of the off-hand available fitting procedures is presented in Sect. 3.8 of this work where, so-called, double diode model (DDM) has been used for analysis of the repeatability of the measurement results for two batches of cells.

3.7. Determination of thermal coefficients

The thermal coefficients of V_{OC} (β), I_{SC} (α) and P_m (power at the maximum power point of I–V curve) are very important parameters (especially those of P_m and V_{OC}) of any PV device since they are indispensable for prediction device performance in realistic operating conditions. Unfortunately, the European standard IEC 60904-5 [4] recommends procedure to determine only the coefficient β .

To enable us routine determination of all three thermal coefficients, a special system for heating/cooling measuring table has been developed at the SolarLab’s setup. The system consists of four water-cooled Peltier cells mounted on the rear side of the measuring table. Depending on a direction of the biasing current flow, the table may be either heated or cooled in the temperature range ~ 0 – 60°C . Gradient of the temperature changes is controlled by a microprocessor system developed at the SolarLab especially for this purpose. After setting the required range and gradient of temperature change, the system works independently of the PC controlled part of the whole setup and thermal coefficients are determined automatically in the preset temperature range without a need of the operator’s intervention.

Figure 10 presents the examples of measurements carried out to determine β and α coefficients. In

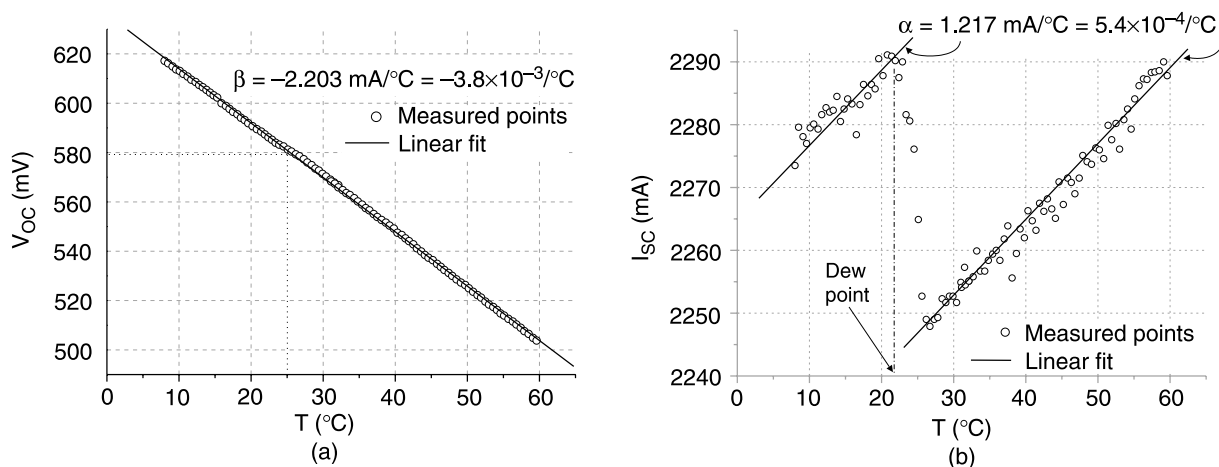


Fig. 10. Examples of thermal coefficients of V_{OC} (a) and I_{SC} (b) determined for multicrystalline Si cell; relative values of coefficients refer to the values measured at 25°C ; note sharp change in I_{SC} when temperature of the measuring table passes dew point.

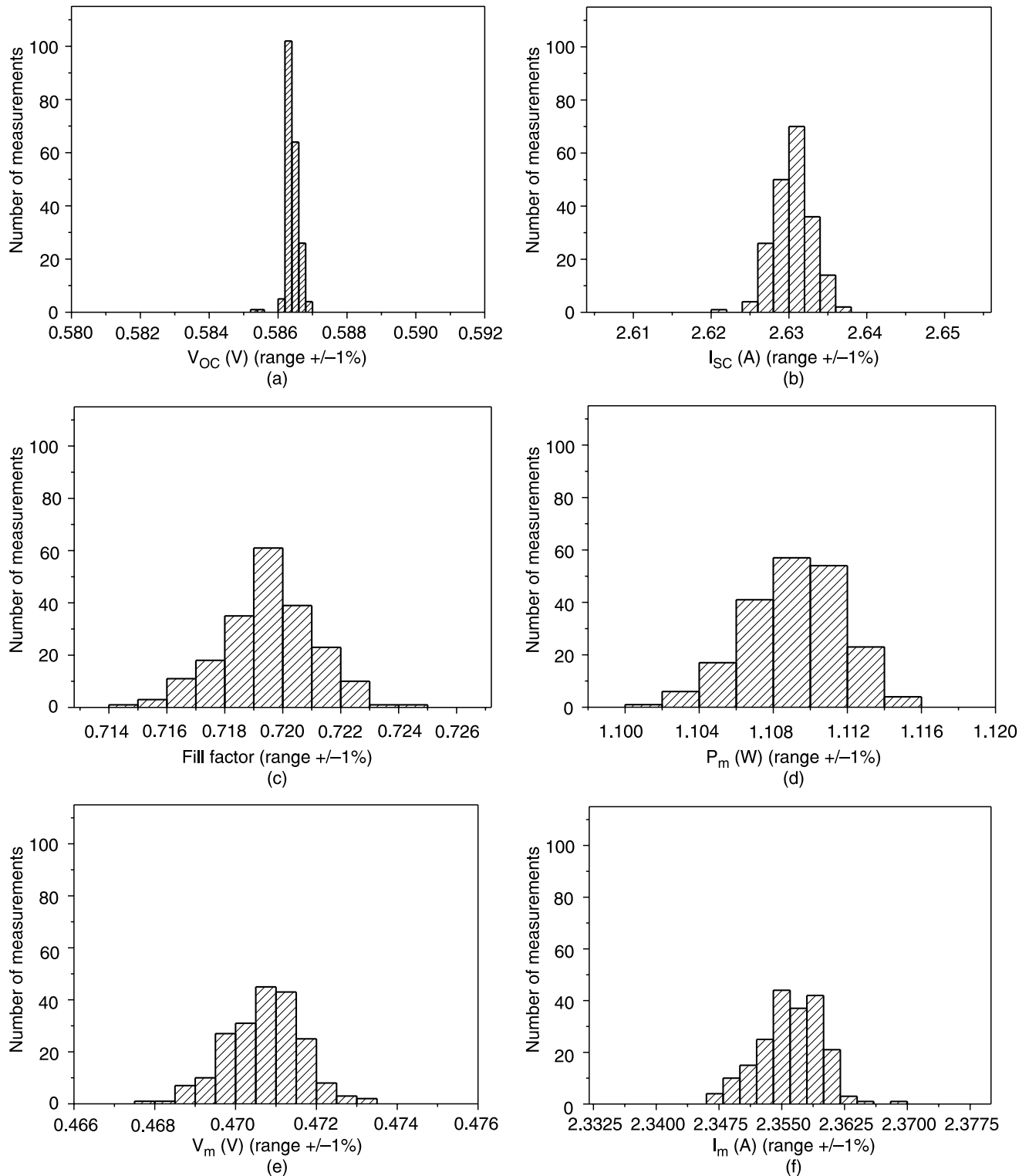


Fig. 11. Distribution of basic parameters of the same cell measured 200 times in 20 s intervals; for better simulation of the routine test of the solar cells batch, measuring probes were raised and cell was not sucked to the table between consecutive I-V scans.

Fig. 10(b), a dew point effect is visible when water vapour condensing on the cell's surface strongly affected its short-circuit current. Very good linearity of both plots makes the determined values of thermal coef-

ficients very reliable. High resolution and accuracy of measurements is particularly well confirmed in the case presented in Fig. 10(b) where α parameter is only 0.0005/°C.

3.8. Repeatability of the measurement results

In the complex system for I–V curves measurement, good repeatability of the measurement results may confirm not only quality of electronic circuits of the measuring unit or stability of light intensity but it also shows if mechanical parts (e.g., probes) applied in the system work correctly and allows for verification of correctness of at least some of numerical procedures applied in the software. Satisfactory repeatability is a feature which is equally important in both laboratory and industrial applications.

To check repeatability of measurement results for the system developed at the SolarLab, 200 measurements have been consecutively carried out for the same cell in 20 second intervals. To eliminate possible increase in temperature of the measuring table, each I–V curve was automatically corrected to the standard test conditions immediately after the scan (see Sect. 3.5).

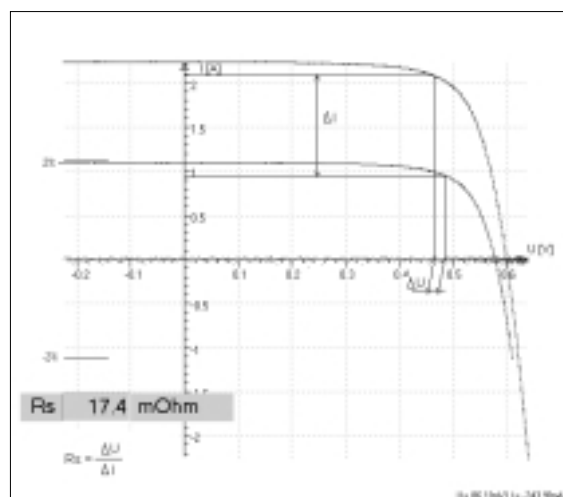
Figure 11 presents distribution of the basic cell's parameters showing excellent repeatability in each case. The largest spread of the data could be observed for P_m and FF (I–V curve fill factor) but still it was in the range $\approx \pm 0.7\%$. The spread of V_{OC} data was in the range ± 1 mV which is better than $\approx \pm 0.2\%$ and I_{SC} lower than ± 10 mA, i.e., less than $\pm 0.35\%$.

4. Determination of the lumped series resistance of solar cells

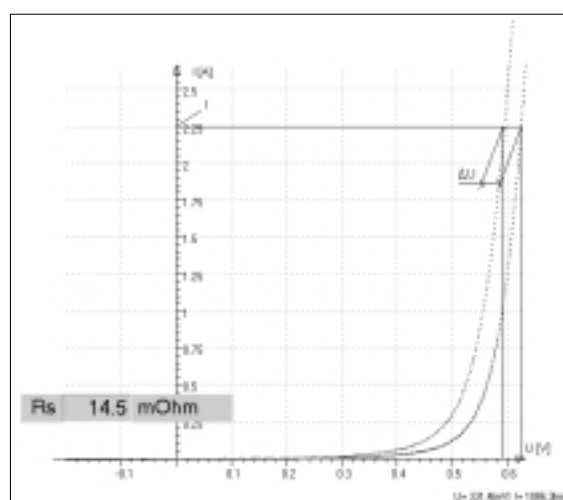
Determination of the lumped series resistance R_S of a solar cell is important since it may be a source of a dominant loss mechanism. The developed system enables us determination of R_S using either of four implemented algorithms including numerical fitting described in Sect. 3.6. Figure 12 presents application of three graphical methods based either on combination of two “light” I–V curves [6] or combination of “dark” and “light” curves [5] or using characteristic bending of the “dark” curve in the high current range of the forward biased cell. All of these methods are off-hand available in the system menu. Discussion concerning the possible errors resulting from using different graphical algorithms may be found in the work of Aberle *et al.* [5]. Figure 13 presents distribution of the cell's lumped series resistance determined using all implemented algorithms for two batches of cells manufactured in the Photovoltaic Lab in Kozy (Poland). As it can be seen though distribution of R_S value within each method is relatively narrow, yet difference in R_S resulting from applying various algorithms may be quite large. The narrower distribution range in both cases could be observed for numerical fitting confirming usefulness of this option.

5. Dark measurements

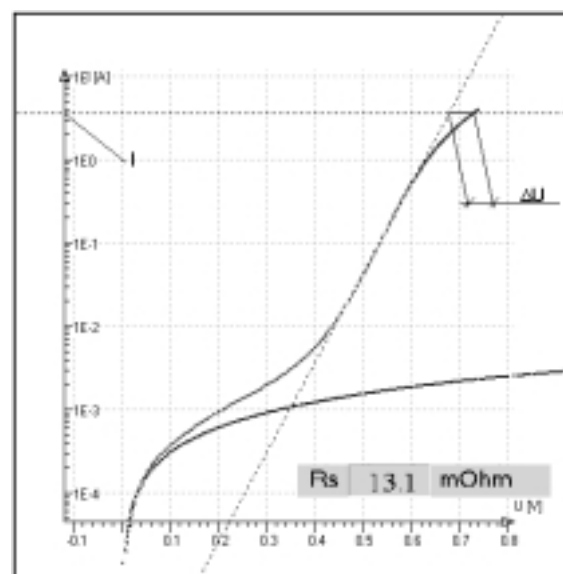
Dark measurements are not very common when characterising solar cells. It has been proved that they may be a very useful tool for analysis of physical processes taking place in photovoltaic devices or for extracting parameters of the



(a)



(b)



(c)

Fig. 12. Graphical procedures used to determine lumped series resistance of a solar cell: IEC 60891 method (after Ref. 6) (a), combination of dark and light measurements (after Ref. 5) (b), using only dark I–V curve (c).

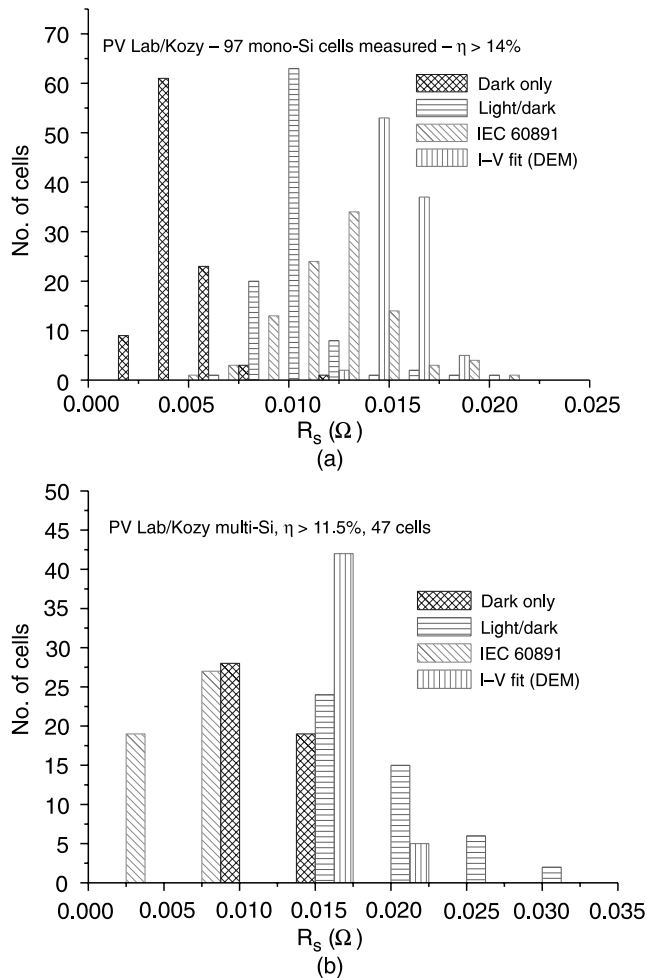


Fig. 13. Distribution of cell's lumped series resistance determined using graphical algorithms presented in Fig. 12 and numerical fitting (sect. 3.6); for experiment two batches of 97 single crystal Si cells (a) and 47 multicrystalline Si cells (b), respectively, manufactured at the Photovoltaic Lab in Kozy (Poland) were used.

equivalent diode model [11,12]. "Dark" I-V curve may be also used directly to determine lumped series resistance of a cell [see Fig. 12(c)]. The option for measurement of "dark" I-V characteristics of the solar cells has been also provided in the SolarLab's system. Very wide range of measurement makes possible to practically characterise all kinds of cells in both forward and reverse bias. During the curve scan, the current range is automatically changed to ensure the highest 16-bit resolution. An example of such a measurement carried out up to 20 A over six orders of magnitude for the high quality standard 10×10 cm² Si cell is shown in Fig. 14. In the lower graph, both reverse and forward parts of the I-V characteristics were plotted in semi-logarithmic scale.

6. Conclusions

The presented results prove usability of the system developed at the SolarLab for the advanced research work. Additionally, the range of measurements and results of the

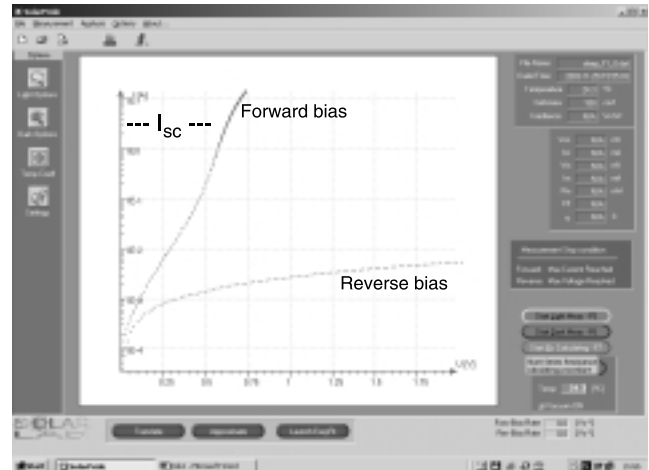


Fig. 14. Example of "dark" I-V curves (screen views) measured up to 20 A over almost six orders of magnitude plotted in semi-logarithmic scale; both forward as well as reverse parts of the curve may optionally be plotted also in linear scale; note that for good quality cell ($R_s < 0.5 \text{ cm}^2$) characteristic curve bending due to cell's series resistance may not be clearly visible until forward current will not be much higher than value of I_{SC} corresponding to standard AM1.5 irradiation ($\sim 2.8 \text{ A}$ in the case).

tests on repeatability, accuracy, and rate of I-V scan when compared to many other systems offered currently on the PV market [13] show that the system can be suitable tool for industrial applications as well.

As it was presented and discussed in Sect. 3.2, the problem related to the cell's heat up effect causing an error in V_{OC} determination, though exists, may be controlled and reduced to acceptable level or, if necessary, it may be even corrected by a proper software procedure.

The other argument, which is quite commonly raised against using continuous light solar simulators on the production line, is a lifetime of the short arc Xenon lamps usually limited to 1000–1500 hours. However, this argument does not really seem to be justified. As it may be easily estimated, at the assumed production throughput 1200 cells/h, more than 1 000 000 measurements may be carried out before a lamp replacement becomes necessary. In fact, for the equipment like SS150, it can be even more because, as it was mentioned in sect. 2.1, when the shutter is closed between the measurements, power supply sets lamp's current on the level much lower than the rated current and hence one may expect the increased lifetime of the lamp.

One can look at the problem also from the point of view concerning the cell production costs. According to the survey made by experts of the PHOTON International Magazine [13], maximum number of flashes for most simulators based on flash lamps fall in a wide range between 40 000 and 1 000 000 which are the values much lower or, in the best case, comparable to the maximum number of measurements that can be done with steady light simulators between necessary lamp replacements. The cost of lamp replacement, with an assumed price of a short arc Xe lamp around 500 €, gives an average cost per single measure-

ment less than 0.0005 /cell corresponding to ~ 0.0002 /Wp for the standard $15 \times 15 \text{ cm}^2$ Si cells.

The systems with steady light simulators do not exhibit also other problems common for measurements with flash simulators like distortion of I–V curve due to capacitance effects or necessary curve correction if scan duration is too long.

Acknowledgements

In its major part, this work was supported by the Polish State Committee for Scientific Research (KBN) within the topic no. 4 of grant PBZ 05/T11/98. The presented exemplary tests on the system performance have been carried out using several hundreds of multicrystalline and single crystal silicon cells developed at the Photovoltaic Laboratory in Kozy, within the topics no. 1 and no. 2 of the same project.

The authors would like to express their gratitude to Tom Moriarty from NREL for making calibration of the cells, Henryk Roguszczyk for making electronic load and Grzegorz Klubinski and Mr. Kamil Wisniewski for making the system to control temperature of the measuring table.

References

1. IEC 60904-1, Photovoltaic devices – Part 1: Measurement of PV current-voltage characteristics.
2. IEC 60904-3, Photovoltaic devices – Part 3: Measurement principles for terrestrial photovoltaic (PV) solar devices with reference spectral irradiance data.
3. IEC 60904-9, Photovoltaic devices – Part 9: Solar simulator performance requirements.
4. IEC 60904-5, Photovoltaic devices – Part 5: Determination of the equivalent cell temperature (ECT) of photovoltaic devices by the open-circuit method.
5. A.G. Aberle, S.R. Wenham, and M.A. Green, “A new method for accurate measurements of the lumped series resistance of solar cells”, *Proc. 23rd IEEE PV Solar Energy Conf.*, 133–139 (1993).
6. IEC 60891, Procedures for temperature and irradiance corrections to measured I–V characteristics of crystalline silicon photovoltaic devices.
7. G. Blaesser and E. Rossi, “Extrapolation of outdoor measurements of PV array I–V characteristics to standard test conditions”, *Solar Cells* **25**, 91–96 (1988).
8. A.J. Anderson, “Photovoltaic translation equations. A new approach”, Subcontract No. TAD-4-14166-01, Final Subcontract Report No. NREL/TP-411-20279, NREL, Jan. 1996.
9. S. Coors and M. Boehm, “Validation and comparison of curve correction procedures for silicon solar cells”, *Proc. 12th EC PV Solar Energy Conf.*, Amsterdam, 1311–1314 (1994).
10. T. Zdanowicz, “Interactive computer program to fit I–V curves of solar cells”, *Proc. 12th EC PV Solar Energy Conf.*, Amsterdam, 131–1314 (1994).
11. J. Beier and B. Voss, “Humps in dark I–V curves – analysis and explanation”, *Proc. 23rd IEEE PV Solar Energy Conf.*, 321–325 (1993).
12. M. Pellegrino, G. Flamini, A. Sarno, and J. Zhao, “Dark measurements technique for PV modules quality evaluation”, *Proc. 17th EC PV Solar Energy Conf.*, 732–735 (2001).
13. “Market survey on cell testers and sorters”, *PHOTON International. The Photovoltaic Magazine* **10**, 48–57 (2002).

Physics and Applications of Optoelectronic Devices (OE104)

Part of SPIE's International Symposium on Optics East
25-28 October 2004 • Pennsylvania Convention Center • Philadelphia, PA, USA

Conference Chair: **Joachim Piprek**, Univ. of California/Santa Barbara

Program Committee: **Jens Buus**, Gayton Photonics Ltd. (United Kingdom); **Silvano Donati**, Univ. degli Studi di Pavia (Italy); **Archie L. Holmes, Jr.**, Univ. of Texas/Austin; **David McDonald**, Intune Technologies (Ireland); **Richard P. Ratowsky**, Finisar Corp.; **Klaus P. Streubel**, OSRAM Opto Semiconductors GmbH (Germany); **Chi-Kuang Sun**, National Taiwan Univ. (Taiwan)

The integration of photonics and electronics in compact optoelectronic devices has greatly benefited many application areas, such as telecommunication, sensing, optical data storage, imaging, and lighting. Explosive developments in several of these areas have significantly increased the demands on the performance of active components. Sophisticated nanometer scale structures are now at the heart of many modern devices. This conference covers various aspects of research and development in optoelectronics: new materials and device designs, modeling and simulation, fabrication and characterization methods, as well as device integration in systems and applications. We strongly encourage researchers, engineers, and product developers across multiple application areas to submit their recent results and to discuss the best approaches to next-generation devices and systems.

Devices and applications of interest include, among others:

- nanostructure devices that facilitate the interaction of electrons and photons
- vertical-cavity surface-emitting lasers for short and long wavelengths
- wavelength tunable laser diodes for sensing, instrumentation, and metrology
- visible and ultraviolet light-emitting devices for lighting, sensing, and data storage
- high-speed photodiodes and arrays for sensing and imaging
- optoelectronic integrated circuits for miniaturization of system functions
- photomixing for mm-wave generation and detection
- single-photon emitters and detectors for quantum cryptography
- mid-infrared semiconductor optoelectronics for sensors
- THz emitters and T-ray imaging
- polymer-based optoelectronic devices for displays
- optoelectronic space and time switches
- reliability and performance improvements.

Abstract Due Date: 12 April 2004
Manuscript Due Date: 27 September 2004



SPIE—The International Society for Optical Engineering is dedicated to advancing scientific research and engineering applications of optical, photonic, imaging, and optoelectronic technologies through its meetings, education programs, and publications.